Liquid Crystals
Publication details, including instructions for authors and subscription information:
http://www.informaworld.com/smpp/title~content=t713926090

Nano-segregated structures of hydrogen-bonded mesogens with perfluorinated moieties: cubic phase formation and first order smectic A to smectic C phase transition

Etsushi Nishikawa Corresponding author[a]; Jun Yamamoto[a]; Hiroshi Yokoyama[ab]
[a] Yokoyama Nano-structured Liquid Crystal Project, Japan Science and Technology Corporation, TRC, Tsukuba, Ibaraki 300-2635, Japan [b] Nanotechnology Research Institute, National Institute of Advanced Industrial Science and Technology, Tsukuba, Ibaraki 305-8568, Japan

Online publication date: 19 May 2010

To cite this Article Nishikawa Corresponding author, Etsushi , Yamamoto, Jun and Yokoyama, Hiroshi(2003) 'Nano-segregated structures of hydrogen-bonded mesogens with perfluorinated moieties: cubic phase formation and first order smectic A to smectic C phase transition', Liquid Crystals, 30: 7, 785 — 798
To link to this Article: DOI: 10.1080/0267829032000093081
URL: http://dx.doi.org/10.1080/0267829032000093081

LIQUID CRYSTALS, VOL. 30, NO. 7, JULY, 2003, 785–798

Taylor & Francis
Taylor & Francis Group

Nano-segregated structures of hydrogen-bonded mesogens with perfluorinated moieties: cubic phase formation and first order smectic A to smectic C phase transition

ETSUSHI NISHIKAWA*†, JUN YAMAMOTO† and HIROSHI YOKOYAMA†‡

†Yokoyama Nano-structured Liquid Crystal Project, Japan Science and Technology Corporation, TRC, 5-9-9 Tokodai, Tsukuba, Ibaraki 300-2635, Japan

‡Nanotechnology Research Institute, National Institute of Advanced Industrial Science and Technology, 1-4-4 Umezono, Tsukuba, Ibaraki 305-8568, Japan

(*Received 25 September 2002; in final form 23 February 2003; accepted 25 February 2003*)

Two series of mesogenic compounds having both a perfluorinated substituent and a hydrogen bonding active site were synthesized and their phase behavior investigated. Due to the chemical architecture of these materials exhibiting amphiphilic character, structures of nano-segregation are expected to form. We found a thermotropic cubic phase with *Ia*3*d* symmetry in one of the acid/base hydrogen-bonded complexes, which is a nano-segregated structure. Moreover materials exhibiting a first order smectic A to smectic C phase transition were found, which was ascertained by differential scanning calorimetry measuring a large latent heat, and X-ray diffraction experiments observing abrupt changes of physical properties at the phase transition, *i.e.* the tilt angle, the intensity and the half-width of the small angle reflection. This first order phase transition occurs due to the frustration of nano-segregated structures of lamellar phases.

1. Introduction

The self-organization of amphiphilic mesogens consisting of two moieties of different chemical nature, *e.g.* hydrophilic/hydrophobic, stiff/flexible, polar/non-polar, and aliphatic/polyaromatic, *etc.*, has been intensively investigated in the last two decades. Due to the high incompatibility between two molecular parts, liquid crystalline phases with intriguing nano-segregated/micro-separated structures have been found to form; for instance, cubic phases with bicontinuous network structure, segregated columnar phases or lamellar phases of well defined sub-layers [1]. Moreover the fluorophilic/fluorophobic interaction among perfluorinated chains and hydrocarbon moieties has also been recognized to promote the self-assembling of molecules [2]. Indeed this effect is successfully used for self-organization leading to intriguing liquid crystalline supramolecular structures, *e.g.* rectangular columnar phases with *c*2*mm* and *p*2*gg* symmetry, or laminated smectic phases [3]. Another important non-covalent force for self-organization to well defined supramolecular structures is hydrogen bonding, which has recently been used to develop new classes of liquid crystalline materials, from low molecular mass to polymeric [4, 5].

In this study we have synthesized two series of materials, which have both a perfluorinated substituent and a site capable of forming hydrogen bonding; thus two important non-covalent interactions, *i.e.* fluorophilic/fluorophobic and hydrogen bonding, can effect and enforce the formation of liquid crystalline phases with nano-segregated structure. We have found in one of the acid/base complexes under investigation—shown in scheme 1(*a*)—the formation of a cubic phase having a bicontinuous network structure of *Ia*3*d* symmetry, which is a nano-segregated structure [6]. In another complex—scheme 1(*b*)—a first order smectic A to smectic C phase transition has been observed, which occurs due to the frustration of liquid crystalline nano-segregated structures [7]. We describe the syntheses and phase behaviour of the studied materials in detail, and discuss the chemical prerequisite to the formation of thermotropic cubic phases, and the phase transition phenomenon between

*Author for correspondence;
e-mail: e2nishik@nanolc.jst.go.jp

Liquid Crystals ISSN 0267-8292 print/ISSN 1366-5855 online © 2003 Taylor & Francis Ltd
http://www.tandf.co.uk/journals
DOI: 10.1080/0267829032000093081

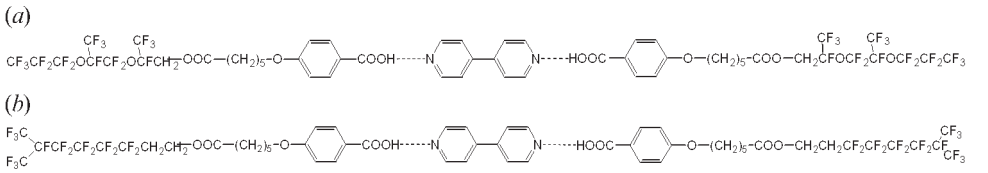

Scheme 1. Chemical structure of the acid/base complexes under investigation. (*a*) **4$_2$-DiPy**; (*b*) **4$_1$-DiPy**.

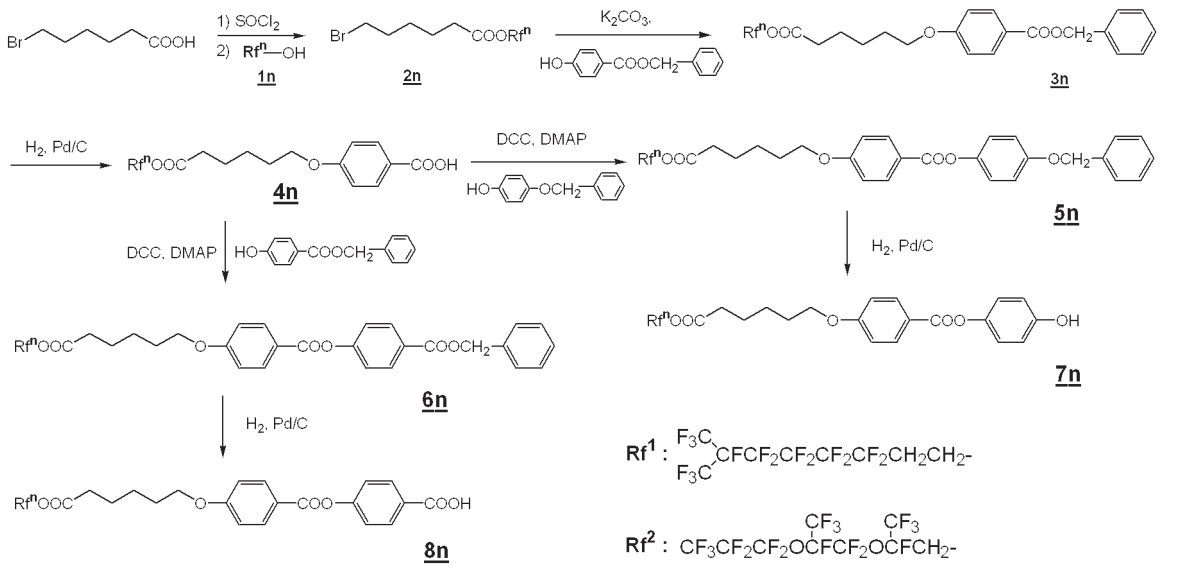

Scheme 2. Synthesis route and chemical structure of the compounds under investigation.

the smectic A phase and the smectic C phase, in connection with microstructural changes.

2. Synthesis

The synthesis route to the compounds under investigation (**4$_n$**–**8$_n$**) is shown in scheme 2. The compounds **4$_n$** are benzoic acid derivatives having either an end-branched perfluoroalkyl chain (*Rf*^{1}–) in the case of **4$_1$** or a relatively bulky perfluorinated substituent (*Rf*^{2}–) for **4$_2$**. Because of the carboxy group these compounds can exist in dimers through hydrogen bonding or form acid/base complexes with basic compounds such as pyridine [8]. The elongation of aromatic parts of **4$_n$** was carried out by the coupling reaction using dicyclohexylcarbodiimide (DCC) and dimethylaminopyridine (DMAP) with either 4-(benzyloxy)phenol or benzyl 4-(hydroxy) benzoate resulting in **5$_n$** or **6$_n$** (**n** = 1, 2). On performing the hydrogenation of **5$_n$** or **6$_n$**, either **7$_n$** having a free hydroxy group, or **8$_n$** having a free carboxy group as a hydrogen bonding active site, were obtained. The detailed procedures of the syntheses are described in § 6.

3. Results

Phase behaviour of the compounds under investigation was determined by polarizing optical microscopy (POM), differential scanning calorimetry (DSC) and X-ray diffraction (XRD), the results summarized in tables 1–3, together with enthalpy changes. Note that

Table 1. Phase transition temperatures (°C) and enthalpy changes [kJ mol^{-1}] of the Rf^1-Series compounds on heating. Cr = crystalline; SmC = smectic C; SmA = smectic A; I = isotropic.

Compound	Cr		SmC		SmA		I
4$_1$	•	87 [17]	•	142 [11.4]	—		•
5$_1$	•	86 [24.5]	•	110 [-]	•	142 [9.3]	•
6$_1$	•	90 [45.9]	{•	58 [-]	•	90 [7.1]}[a]	•
7$_1$	•	98 [34.9]	•	112 [4.7]	—		•
8$_1$	•	133 [10.1]	•	223 [18.2]	—		•

[a]Monotropic transition.

Table 2. Phase transition temperatures (°C) and enthalpy changes [kJ mol^{-1}] of the Rf^2-Series compounds on heating. Cr = crystalline; SmC = smectic C; SmA = smectic A; I = isotropic.

	Cr		SmC		SmA		I
4$_2$	•	−5 [19.6]	•	108 [5.5]	—		•
5$_2$	•	46 [26.9]	•	135 [8.6]	—		•
6$_2$	•	52 [39]	•	69 [0.13]	•	84 [3.4]	•
7$_2$	•	61 [9.3]	•	88 [1.6]	•	96 [0.7]	•
8$_2$	•	101 [4.4]	•	218 [11.2]	—		•

Table 3. Phase behaviour of 4,4′-dipyridyl (**DiPy**) complexes of $\mathbf{4}_n$ compounds. Cr_1, Cr_2 = crystalline; Sm = smectic; SmC = smectic C; SmA = smectic A; Cub = cubic; Col = columnar; I = isotropic.

Acid	Base	Phase transition temperatures/°C [enthalpy/kJ mol^{-1}]								
$\mathbf{4_1}$	**DiPy**	Cr_1	87	Cr_2	106 [39.2]	SmC	157 [5.3]	SmA	161 [13.1]	I
$\mathbf{4_2}$	**DiPy**	Cr	69 [9.7]	Sm	91 [2.1]	Cub	138 [0.6]	Col	139 [2.1]	I

the values of enthalpy change were determined as those of monomer forms although $\mathbf{4}_n$, $\mathbf{7}_n$ and $\mathbf{8}_n$ can exist in elongated dimer forms through hydrogen bonding. The enthalpy changes of the 4,4′-dipyridyl complexes were evaluated as those of the hydrogen-bonded complexes.

3.1. *Phase behaviour of the neat materials*

3.1.1. *Phase behaviour of* $\mathbf{4}_n$

Both the neat acids show only one liquid crystalline (LC) phase, a smectic C (SmC) phase. The acid $\mathbf{4_1}$, having an end-branched perfluoroalkyl chain, melts at 87°C into a SmC phase, which transforms into an isotropic (I) liquid at 142°C with an enthalpy change (ΔH) of 11.4 kJ mol^{-1}. The acid $\mathbf{4_2}$ melts at −5°C into a SmC phase, which persists until an I phase transition takes place at 108°C with ΔH of 5.5 kJ mol^{-1}. Owing to the bulky flexible perfluorinated moiety the melting temperature of $\mathbf{4_2}$ is relatively low compared with that of $\mathbf{4_1}$.

3.1.2. *Phase behaviour of* $\mathbf{5}_n$

The benzyl ester derivatives $\mathbf{5}_n$, *i.e.* the precursors to $\mathbf{7}_n$, have no hydrogen bonding active site. $\mathbf{5_1}$ melts at 86°C to form a SmC phase, which transforms into a smectic A (SmA) phase at 110°C, followed by an I phase transition at 142°C. On cooling, the SmC phase is supercooled to 60°C. The SmA to SmC phase transition of this material is observed with POM, but not with DSC. $\mathbf{5_2}$ shows only a SmC phase in the temperature range 46–135°C. On cooling, a supercooling of the SmC phase occurs, with crystallization at 37°C.

3.1.3. *Phase behaviour of* $\mathbf{7}_n$

This series of compounds has a phenol group capable of hydrogen bonding. $\mathbf{7_1}$ exhibits only a SmC phase between 98 and 112°C. On cooling, the SmC phase is supercooled until crystallization occurs at 66°C. $\mathbf{7_2}$ melts at 61°C into a SmC phase, which transforms to a SmA phase at 88°C. The SmA to SmC phase transition is observed by POM and also by DSC, measuring a ΔH of 1.6 kJ mol^{-1}. This latent heat is relatively large for a SmA to SmC phase transition. The SmA to I phase transition occurs at 96°C with ΔH of 0.7 kJ mol^{-1} (entropy change $\Delta S = 1.9$ J mol^{-1} K^{-1}), which is remarkably small for a SmA to I phase transition.

3.1.4. *Phase behaviour of* $\mathbf{6}_n$

The benzyl ester derivatives $\mathbf{6}_n$ that are the precursors to $\mathbf{8}_n$, exhibit both a SmA phase and a SmC phase. $\mathbf{6_1}$ monotropically shows a SmA phase and a SmC phase on cooling; that is, the SmA phase appears at 90°C and transforms into the SmC phase at 58°C which exists until crystallization occurs at 42°C. The SmA to SmC phase transition is observed with POM but not with DSC. On heating, a crystalline to crystalline transition occurs at 53°C and then the crystal melts at 90°C directly into the I phase. $\mathbf{6_2}$ melts at 52°C into a SmC phase and transforms to a SmA phase at 69°C, followed by an I phase transition at 84°C. The SmA to SmC phase transition of this material is slightly detected with DSC, showing ΔH of 0.13 kJ mol^{-1}. On cooling the SmC phase is supercooled to about 20°C.

3.1.5. *Phase behaviour of* $\mathbf{8}_n$

The organic acids $\mathbf{8}_n$ are two ring systems having a carboxy group at one end, and can form dimeric structures through hydrogen bonding. $\mathbf{8_1}$ exhibits only a SmC phase between 133 and 223°C, while $\mathbf{8_2}$ shows a SmC phase between 101 and 218°C. The clearing temperatures of $\mathbf{8}_n$ are considerably higher compared with those of $\mathbf{7}_n$ having a phenol group as a hydrogen bonding active site. This result suggests that $\mathbf{8}_n$ exists in dimer forms because the hydrogen bonding is strong enough, while in case of $\mathbf{7}_n$ the hydrogen bonding is too weak to stabilize a linear dimeric structure.

3.2. *Phase behaviour of the 4,4′-dipyridyl hydrogen-bonded complexes of* $\mathbf{4}_n$ *(*$\mathbf{4}_n$***-DiPy**)*

The hydrogen-bonded 4,4′-dipyridyl (**DiPy**) complex of $\mathbf{4_1}$ ($\mathbf{4_1}$**-DiPy**, see scheme 1*b*) melts at 106°C into a SmC phase. Then a SmA to SmC phase transition occurs at 157°C, followed by an I phase transition at 161°C. Figure 1 shows polarized optical photomicrographs of the $\mathbf{4_1}$**-DiPy** complex sandwiched between two normal glass plates (*a*) and (*b*) or two polyimide-coated glass plates (*c*) and (*d*). Figure 1 (*a*) is taken at the SmA to SmC phase transition temperature, showing two regions: one dark region showing homeotropical uniform molecular alignment of the SmA phase, and another showing schlieren texture of the SmC phase. Figure 1 (*b*) demonstrates the SmA to I phase transition

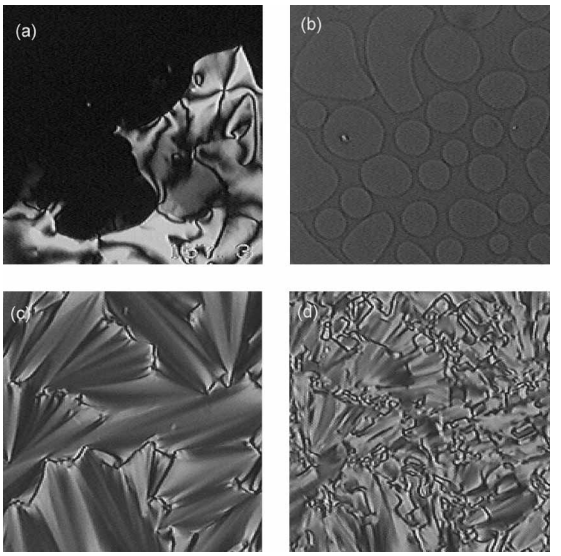

Figure 1. Polarized optical photomicrographs of the hydrogen-bonded complex **4_1-DiPy**: (*a*) at 157°C showing the SmC (schlieren texture) to SmA (homeotropic alignment) phase transition; (*b*) at 161°C showing the isotropic phase transition observed between non-coated glass plates; (*c*) at 160°C showing focal-conic texture of the SmA phase; (*d*) at 156°C showing the broken texture of the SmC phase observed between polyimide-coated glass plates.

that appears to occur like a two-phase separation. Note that at the boundaries of two phases no birefringence appears, indicating completely homeotropical molecular orientation in the SmA phase. Figure 1 (*c*) shows a typical fan-shaped texture of the SmA phase, while figure 1 (*d*) shows a broken texture of the SmC phase. These two textures, (*c*) and (*d*), are observed to change reversibly with increasing and decreasing temperature.

A DSC thermogram of **4_1-DiPy** is shown in figure 2 (*a*), in which the SmA to SmC phase transition is clearly observed as a sharp peak. The enthalpy change of the SmA–SmC phase transition amounts to $5.3\,\mathrm{kJ\,mol^{-1}}$ ($\Delta S = 12.3\,\mathrm{J\,K^{-1}\,mol^{-1}}$), which is a vast amount of latent heat for SmA to SmC phase transition. This result is indicative of a first order phase transition.

The complex **4_2-DiPy** between **4_2** and 4,4′-dipyridyl see scheme 1(*a*) is found to organize in a thermotropic cubic (Cub) phase. A DSC thermogram measured at a heating/cooling rate of $2\,\mathrm{K\,min^{-1}}$ is shown in figure 2 (*b*). A crystalline to crystalline phase transition occurs at 38°C and then the crystal melts at 69°C into a LC phase (SmX), which we have not yet assigned. At 91°C a cubic phase transition takes place with ΔH of $2.1\,\mathrm{kJ\,mol^{-1}}$, followed by a columnar phase transition at 138°C with ΔH of $0.6\,\mathrm{kJ\,mol^{-1}}$. An isotropic phase transition is then observed at 139°C with ΔH of

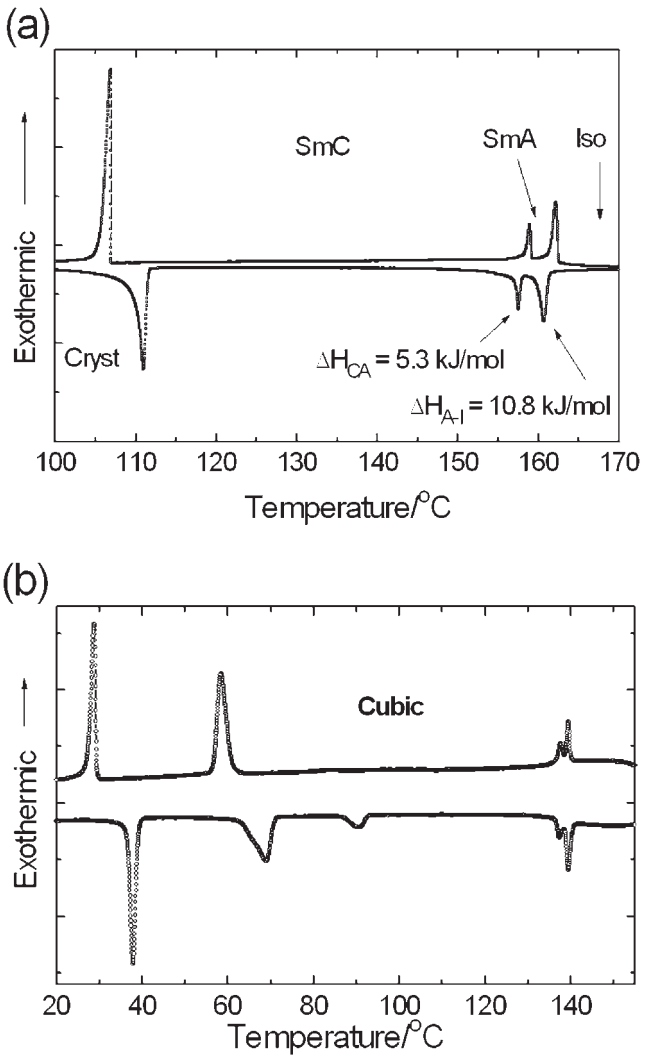

Figure 2. DSC thermograms of the hydrogen-bonded complexes (*a*) **4_1-DiPy** and (*b*) **4_2-DiPy**, observed at a cooling/heating rate of $2\,\mathrm{K\,min^{-1}}$.

$2.1\,\mathrm{kJ\,mol^{-1}}$. On cooling, the Cub phase is supercooled until crystallization occurs at 58°C. In this process the SmX phase does not appear.

4. Discussion

In the previous section we have described the detailed phase behaviour of the compounds under investigation. One hydrogen-bonded complex exhibits a cubic phase (**4_2-DiPy**). One of the subjects of this work is to understand the chemical features of compounds capable of organizing into thermotropic cubic phases; this is discussed in §4.1. Another topic concerns phase transition behaviour between SmA and SmC phases. It has been found that some reported compounds show only a SmC phase while some form both a SmA phase and a SmC phase. In the later case the SmA to SmC

phase transition has been found to occur either as a first order or a second order phase transition depending on the chemical structures of the materials. This phase transition is discussed in § 4.2., in connection with the microstructure changes of lamellar phases at the phase transition.

4.1. *Cubic phase formation*

The 4,4′-dipyridyl complex of **4_2** (**4_2-DiPy**) forms a thermotropic cubic phase. The microstructure of the cubic phase was analysed with XRD. Figure 3 shows an X-ray pattern taken at a temperature of 65°C in the cubic phase on cooling together with the corresponding intensity profile.

Some Bragg-like spots are seen at small angles while a broad isotropic reflection is observed at wide angles. The intensity profile clearly exhibits four kinds of peak with the wave vectors $q_1 = 1.40$, $q_2 = 1.62$, $q_3 = 2.14$ and $q_4 = 2.82\,\mathrm{nm}^{-1}$ ($q = 4\pi\sin\theta/\lambda = 2\pi/d$, 2θ = scattering angle, $d = d$-spacing, $\lambda = 0.154\,\mathrm{nm}$), corresponding to the d-spacings $d_1 = 4.49$, $d_2 = 3.88$, $d_3 = 2.93$ and $d_4 = 2.23\,\mathrm{nm}$, respectively. As the ratio of $q_1 : q_2 : q_3 : q_4$ is $6^{1/2} : 8^{1/2} : 14^{1/2} : 24^{1/2}$, we can index the reflections (2 1 1), (2 2 0), (3 2 1) and (4 2 2), respectively. From this X-ray pattern, the cubic phase of the complex can be assigned to a structure with body-centred cubic symmetry, (*Ia*3*d*), which could be a bicontinuous interpenetrating jointed rod network structure, similar to that discussed in other systems [9–11]. The cell parameter of the cubic phase is estimated as $a = 10.9\,\mathrm{nm}$, which is approximately twice the molecular length of the complex ($l = 5.5\,\mathrm{nm}$). Temperature dependent XRD measurements have revealed that with increasing temperature the unit cell parameter decreases, exhibiting a negative thermal volume expansion of $(1/a^3)[\delta(a^3)/\delta T] = -2.3 \times 10^{-3}\,\mathrm{K}^{-1}$, which is consistent with the values reported in other recent work on compounds showing cubic phases [11, 12].

The optically isotropic phase of 4′-*n*-alkoxy-3′-nitrobipheny1-4-carboxylic acids (abbreviated to **ANBC-*n***, ***n*** is the alkyl chain carbon number) was reported by Gray *et al.* in 1957, and later identified as a liquid crystalline phase with cubic symmetry by Demus *et al.* in 1968 [13, 14]. Since then, thermotropic cubic phases have aroused much interest as their microstructures are intriguing and the presence of the cubic phase between two lamellar phases (SmC and SmA) is curious. During the last two decades, structures of the cubic phases of **ANBC-*n*** have been intensively studied by ^{1}H NMR, ^{13}N NMR, XRD, IR, viscoelastic measurements, dielectric measurements and calorimetric experiments, *etc.* [11, 15–23].

In parallel with the structure analysis on **ANBC-*n*** and on other cubic phase-forming materials, many new materials organizing in optically isotropic phases, *e.g.* polycatenar and swallow-tailed compounds, have been synthesized, and are summarized in recent articles [24, 25]. Furthermore, a variety of new materials with quite different chemical structures have been reported in the last decade, for instance, dichiral compounds [26], dendrimeric compounds [27] and folic acid derivatives [28]. Moreover, polyhydroxy amphiphiles [29], four-ring imines with fluorinated chains [30], hydrogen-bonded siloxane-containing acid/base complexes [31] and coil-rod-coil oligomeric molecules [32], *etc.* have been found to show cubic phases. An important common feature of these materials from the chemical point of view is that they possess amphiphilic character due to two (or three) incompatible compositional moieties. Recently a molecular dynamic simulation on a cubic phase-forming compound, 1,2-bis[4-*n*-octyloxybenzoyl]hydrazine (**BABH8**), was carried out and revealed that the molecule has a strong segregation power between core and tails; this

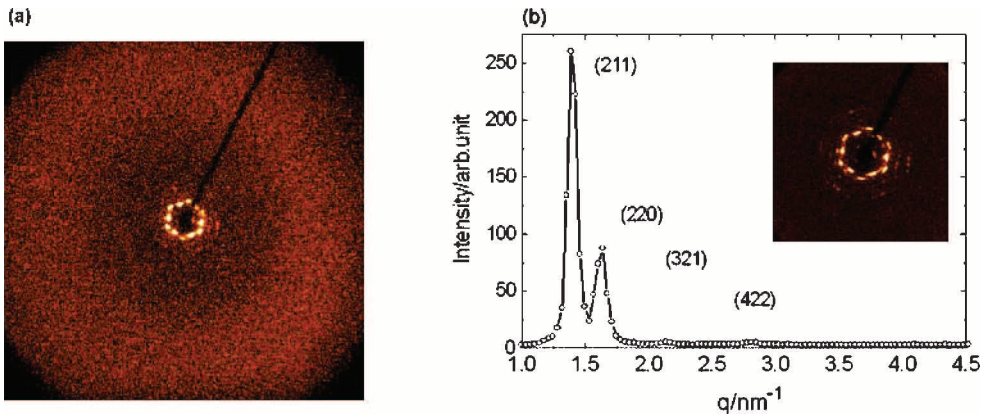

Figure 3. (*a*) X-ray diffraction pattern of **4_2-DiPy** observed in the cubic phase at 65°C; (*b*) the intensity profile at small angles, showing a body-centred cubic symmetry (*Ia*3*d*).

was pointed out to be a crucial factor for cubic phase formation [33].

The acid/base complex **4_2-DiPy** also has an amphiphilic character due to a fluorophilic/fluorophobic interaction, which leads to the formation of segregated microstructures. This feature is thus again an important factor in the organization of cubic phases. However, as described, **4_1-DiPy**, which has a similar chemical architecture to **4_2-DiPy**, does not form cubic phases. Some other materials having a similar chemical structure to **4_1-DiPy** were reported in our previous work, and were also found not to form cubic phases [34]. The significant difference among them is the bulkiness of the perfluorinated moieties. The perfluorinated part of the cubic phase-forming **4_2-DiPy** is much bulkier and more flexible than the perfluorinated parts of the others that do not form cubic phases. This point may be one of the crucial chemical features in the formation of cubic phases.

Another point to note is by that the neat organic acid **4_2** does not form cubic phases, but the acid/base complex **4_2-DiPy** does. This may indicate that the effective length of the mesogenic core is important for cubic phase formation. The dimer form of **4_2** has a three-ring core when the cyclic hydrogen-bonded part is included, which could be too short for cubic phase formation. The cubic phase forming complex **4_2-DiPy** is a four-ring system, which could be more effective in cubic phase formation. Polycatenar compounds and swallow-tailed mesogens, which can form thermotropic cubic phases, also have long aromatic core systems. Therefore one could expect that the organic acid **8_2** could form a cubic phase because it has the same perfluorinated moiety as **4_2-DiPy**, and its elongated mesogenic core structure (through hydrogen-bonding) has a five-ring core—longer than that of **4_2-DiPy** and even as long as **ANBC-*n***. However it has been found that this neat acid does not form cubic phases, but again the acid/base complex between 4,4′-dipyridyl and **8_2** does [35]. These results mean that in the series of compounds investigated in this work the acid/base complexation is crucial to cubic phase formation.

In case of **BABH** the existence of lateral molecular interaction through diimine nitrogen–hydrogen bonding is proposed as a responsible factor in cubic phase formation [36]. In the studied acid/base complexes that have the tendency to form nano-segregated structures, lateral molecular interactions can be promoted by the following two factors. First, 4,4′-dipyridyl can move easily in its micro-segregated domain relative to the domain of the perfluorinated acid, as the hydrogen bonding is dynamic and transient. Second 4,4′-dipyridyl can freely rotate around the molecular long axis of the complex, independent of the acid parts. These two aspects that probably enable and enhance lateral molecular interactions could also be the important factors in cubic phases formation. We are now synthesizing new compounds for the study and understanding of chemical requirements for thermotropic cubic phase formation.

4.2. *Smectic A to smectic C phase transition*

The 4,4′-dipyridyl complex of **4_1** (**4_1-DiPy**) exhibits a SmA to SmC phase transition, which is observed with DSC as a strong peak with the corresponding enthalpy change of $\Delta H = 5.3\,\mathrm{kJ\,mol^{-1}}$. As this amount of latent heat is remarkably large for a SmA to SmC phase transition, the transition of this complex is possibly of first order. In order to characterize the phase transition, temperature-dependent XRD experiments were carried out. The results are summarized in figure 4.

The small angle reflection resulting from the lamellar structure clearly shows that at the SmA to SmC phase transition the wave vector (q-value) changes abruptly. Figure 4 (*b*) shows the corresponding d-spacing change and the tilt angle change calculated from the original XRD data of Figure 1 (*a*). In the SmA phase a layer spacing $d_A = 47.7\,\text{Å}$ is observed, while in the SmC phase at 1°C below the phase transition temperature, a layer spacing $d_{C(T)} = 45.4\,\text{Å}$ is seen. Using the relation $\theta = \arccos [d_{C(T)}/d_A]$, the corresponding tilt angle change of 17.9° is calculated. A large tilt angle at the SmA to SmC phase transition is seen; thereafter the tilt angle increases slightly with decreasing temperature and becomes almost constant. Generally the tilt angle can be regarded as the primary order parameter of the SmA to SmC phase transition [37]. It changes continuously in the case of a second order phase transition, but discontinuously if the transition is of first order. Therefore the observed tilt angle change on the hydrogen-bonded complex suggests that the SmA to SmC phase transition is of first order. Figures 4 (*c*) and 4 (*d*) show the temperature dependence of the intensity and the half-width of the small angle reflection, respectively. The intensity of the small angle reflection discontinuously changes at the SmA to SmC phase transition, probably indicating a discontinuous change of density. The half width, which is related to the correlation length of smectic layers in a direction parallel to the layer normal, is observed to change discontinuously at the SmA to SmC phase transition. These results from XRD experiments also suggest that the SmA to SmC phase transition of **4_1-DiPy** is of first order. So far clear evidence of a first order SmA to SmC phase transition does not appear to have been experimentally observed, except in the homologues of the terephthal-bis-*p*-*n*-alkylaniline series [38]. In relation to the SmA to chiral

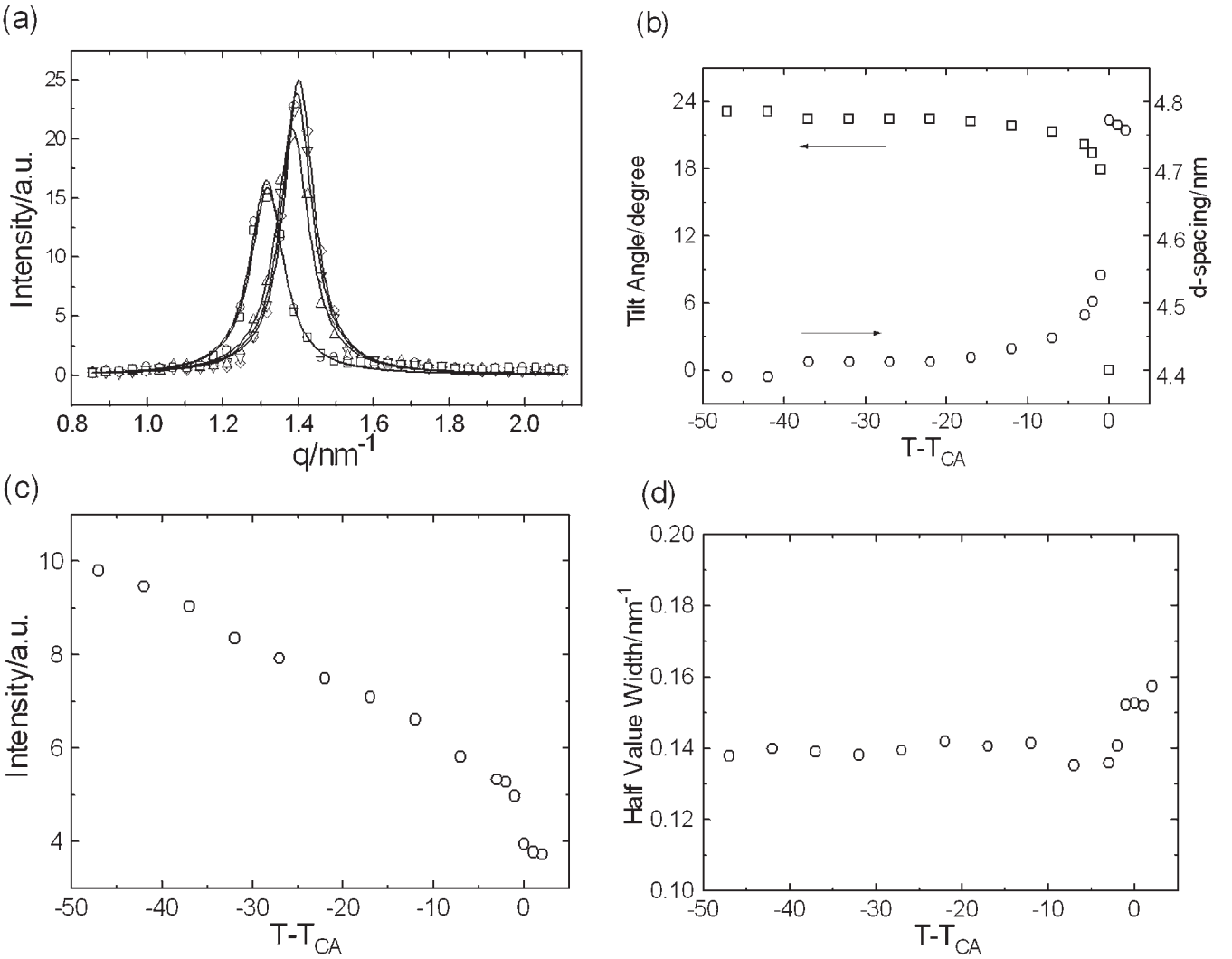

Figure 4. (*a*) Intensity profiles at small angle regions at temperatures of (□) 159°C, (○) 158°C, (△) 157°C, (▽) 156°C and (◇) 155°C; (*b*) (○) temperature dependent *d*-spacing and (□) tilt angle; (*c*) temperature dependent intensity; (*d*) temperature dependent half-width, observed on **4$_1$-DiPy**. *T* denotes the measurement temperature and T_{CA} the SmC to SmA phase transition temperature of 157°C.

smectic C (SmC*) phase transition, Heppke *et al.* [39] reported a compound showing a first order SmA to SmC* phase transition: (*S, S*)-4-(3-methyl-2-chloropentanoyloxy)-4′-heptyloxybiphenyl. This was studied by means of XRD, with theoretical work by Líen and Huang [40]. Thereafter first order SmA to SmC* phase transitions on several compounds have been discussed [41].

We suggest the following reasons why the studied complex shows a first order SmA to SmC phase transition. As mentioned above, the layer *d*-spacing of the SmA phase is 47.7 Å, while the molecular length of the acid/base complex is calculated to be 65 Å. This means that the SmA phase should be partially interdigitated (SmA_d). If the interdigitation between the perfluorinated moieties and the alkyl chain parts shown in figure 5 is assumed in the SmA_d phase, the calculated layer distance becomes about 48 Å, which is consistent with the observed *d*-spacing of 47.7 Å. In this model of the SmA_d phase, therefore, segregation between the perfluorinated chains and the normal alkyl groups does not take place completely; only the aromatic parts elongated through hydrogen bonding are segregated.

However in the SmC phase that appears on lowering the temperature from the SmA_d phase, the favourable segregation of the perfluorinated moieties and the normal hydrocarbon chains possibly occurs as shown in figure 6 (*a*). Recently, Weissflog *et al.* reported that at the smectic to columnar phase transition of perfluorinated swallow-tailed compounds, a change of segregation (interdigitation) could take place [43]. As in

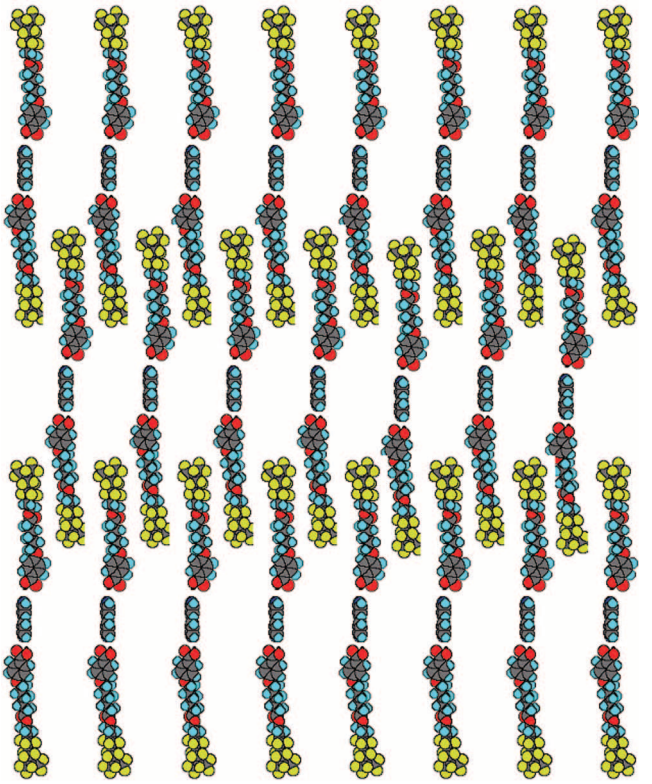

Figure 5. Model of microstructure of the SmA phase of **4_1-DiPy**, showing interdigitation between the perfluorinated moieties (green) and the alkyl chains (blue).

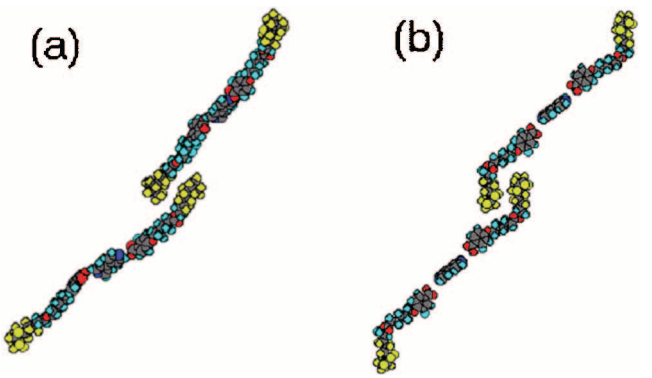

Figure 6. Model of microstructure of the smectic C phase of **4_1-DiPy**, showing (*a*) possible change of the degree of interdigitation, (*b*) possible change of the conformation resulting in a zig-zag conformation, in comparing with the microstructure of the smectic A phase (see figure 5).

this case, it is possible to suppose that in the acid/base complex studied the degree of interdigitation could change at the phase transition. Moreover a change of molecular conformation could take place. At the link between the perfluorinated moiety and the alkyl chain the linear conformation could bend to change into a zig-zag conformation as shown in figure 6 (*b*). Such a zig-zag conformation in smectic phases has recently been examined by Clark *et al.* by means of IR measurements [44], and by Shashidhar *et al.* [45] on siloxane-containing compounds in connection with electroclinic effects and de Vries smectics [46, 47]. In the model of the zig-zag conformation of the complex, the free space among molecules could be more fully filled than in the model of the linear conformation.

We speculate that these possibly occurring microstructural changes could cause a first order SmA_d to SmC phase transition of the complex, which could be supported from the X-ray diffraction data shown in figure 7. In the SmC phase the second and third order small angle reflections of lamellar structure are clearly detected, while these reflections are absent in the SmA_d phase. This indicates that the segregation of the molecular parts becomes more definite in the SmC phase than in the SmA_d phase. At wide angles, a broad reflection at around 0.6 nm ($q \approx 10\,nm^{-1}$) resulting from the perfluorinated parts can be recognized, which reveals the segregation of the perfluorinated moiety. The corresponding intensity appears to be stronger in the SmC phase than in the SmA_d phase, on analysing the fitting data. Moreover the wide angle reflection from the aromatic core part is observed at around 0.54 nm ($q \approx 11\,nm^{-1}$), which is considerably larger than the conventional wide angle reflection at about 0.46 nm ($q \approx 13\,nm^{-1}$). This means that the averaged aromatic core distance is large in the complex, as can be postulated from the models in figure 5. The difference in the observed wide angle reflection pattern between the SmA_d phase and SmC phase suggests that the microstructural changes take place as discussed above.

As described in § 3.1, four of the other compounds under investigation (**5_1**, **6_1**, **6_2** and **7_2**) show both a SmA

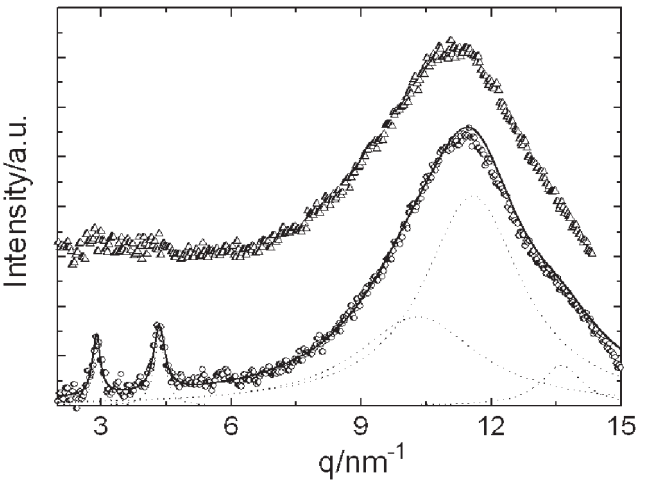

Figure 7. X-ray patterns of **4_1-DiPy** observed (△) at 160°C in the smectic A phase and (○) at 120°C in the smectic C phase. The solid and dotted lines are fittings.

phase and a SmC phase. The SmA to SmC phase transition of $\mathbf{5_1}$ and $\mathbf{6_1}$ was not detected with DSC, while that of $\mathbf{6_2}$ was detected as a small peak with ΔH of 0.13 kJ mol^{-1}. These thermal measurements indicate that the SmA to SmC phase transition of the three compounds is of second order. The SmA to SmC phase transition of $\mathbf{7_2}$ is clearly observed with DSC showing ΔH of 1.6 kJ mol^{-1}. This relatively large latent heat indicates that the phase transition is possibly of first order, similar to that of **4_1-DiPy**. Temperature-dependent XRD experiments were carried out on $\mathbf{7_2}$ and $\mathbf{6_2}$ to study the SmA to SmC phase transition behaviour. The results are shown in figures 8(*a*) and 8 (*b*), respectively. Compound $\mathbf{7_2}$ exhibits a constant *d*-spacing of 41.2 Å in the SmA phase, which decreases steeply at the SmA–SmC phase transition at 88°C and then slightly with further decreasing temperature. The observed tilt angle at 1°C below the phase transition temperature is 8°. Compound $\mathbf{6_2}$ exhibits a *d*-spacing that gradually changes around the SmA to SmC phase transition. Figure 9 summarizes the temperature-dependent tilt angle of the compounds $\mathbf{6_2}$, $\mathbf{7_2}$ and **4_1-DiPy**. As can be seen, the tilt angle change of $\mathbf{7_2}$ around the SmA to SmC phase transition temperature is similar to that of **4_1-DiPy**, while $\mathbf{6_2}$ shows a significantly different behaviour. These results indicate that the SmA to SmC phase transition of $\mathbf{7_2}$ is probably of first order, while that of $\mathbf{6_2}$ is of second order.

As already described, the *d*-spacing of the SmA phase of $\mathbf{7_2}$ is 41.2 Å, while the molecular length is calculated as $l = 31.3$ Å. In order to reconcile these two lengths we propose a model of interdigitated microstructure to the SmA phase (SmA_d) as shown in figure 10. In this model the perfluorinated moieties and the hydrocarbon parts are completely segregated. Hydrogen bonding takes place between the phenol group and the oxygen atom of the ester group that links the alkyl chain to the perfluorinated moiety. In this case, the degree of interdigitation probably does not change at the SmA to SmC phase transition, because favourable space filling and segregation between hydrocarbon and perfluorinated parts are already established. It is reasonable to suppose that a bend at the ester group that links the perfluorinated part to the alkyl chain leads to a zig-zag molecular conformation, resulting in a molecular tilt at the SmA to SmC transition. This could be preferred to the conventional inclination of the whole molecule.

Finally we should describe the SmA to I phase transition of $\mathbf{7_2}$. In the I phase a diffuse small angle reflection is observed by XRD up to a high temperature above the I to SmA phase transition, which indicates

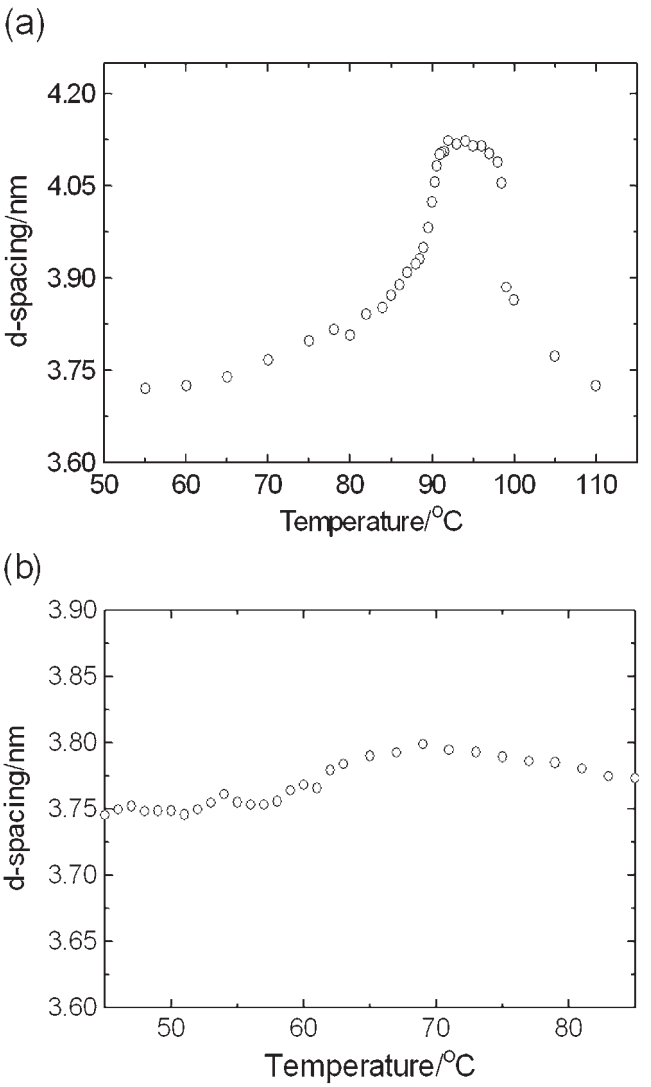

Figure 8. Temperature dependent *d*-spacing changes of (*a*) $\mathbf{7_2}$ and (*b*) $\mathbf{6_2}$, measured by XRD.

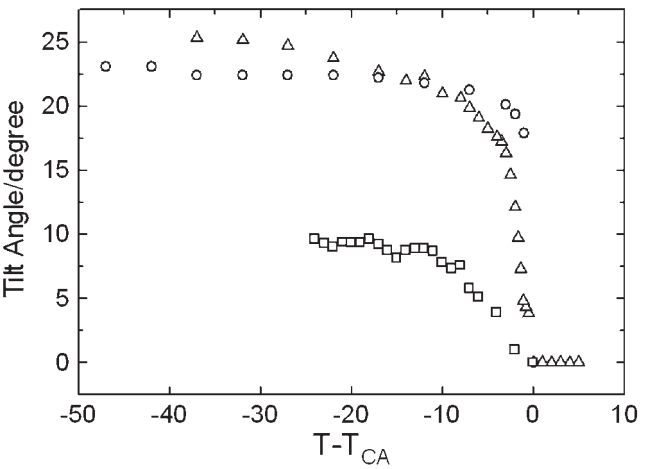

Figure 9. Temperature-dependent tilt angle determined by XRD on (○) **4_1-DiPy**; (△) $\mathbf{7_2}$; (□) $\mathbf{6_2}$.

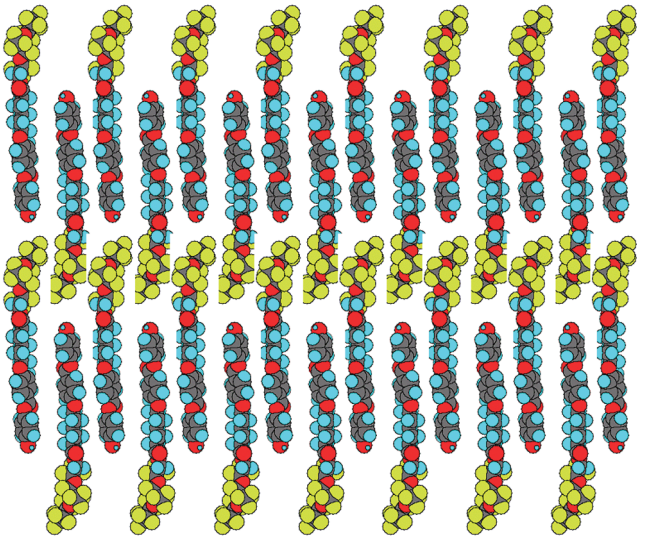

Figure 10. Model of microstructure of the smectic A phase of $\mathbf{7_2}$, showing the interdigitation that leads to complete segregation between the fluorinated moieties and the hydrocarbon parts.

that in the I phase micro-separated structure still exists, probably a kind of aggregate, *e.g.* smectic clusters. As seen in figure 8 (*a*), the calculated *d*-spacing abruptly increases at the I to SmA phase transition with decreasing temperature as a consequence of a first order phase transition. However, as already described, the enthalpy change of the I to SmA phase transition amounts to $\Delta H = 0.7\,\mathrm{kJ\,mol^{-1}}$ (entropy change = $1.9\,\mathrm{J\,mol^{-1}\,K^{-1}}$), which is rather small for a SmA to I phase transition. This could mean that the I to SmA phase transition tends toward a second order transition [48].

5. Conclusions

Two series of new mesogens, with both a perfluorinated substituent and a site capable of hydrogen bonding, have been synthesized in order to study the influence of strong amphiphilic character of the molecules on the formation of liquid crystalline phases with segregated microstructures.

We have found that an acid/base complex between one of the studied organic acids and 4,4′-dipyridyl forms a thermotropic cubic phase with *Ia3d* symmetry; this is a highly self-organized structure with micro-segregation among incompatible constitutional molecular parts. In order to organize the cubic phase, the bulkiness and flexibility of the perfluorinated moiety play important roles, in addition to the segregation power resulting from the fluorophilic/fluorophobic interaction. Moreover the complex formation enables and strengthens lateral molecular interaction, which is crucial for cubic phase formation in the materials studied.

Five compounds under study form both a smectic A phase and a smectic C phase. Two of them were found to show a first order smectic A to smectic C phase transition. The microstructures of both the lamellar phases consist of well defined sub-layers of perfluorinated moieties, hydrocarbon chains or aromatic core parts, which are nano-segregated structures. The first order smectic A to smectic C phase transition occurs owing to the frustration of microstructures between the two phases, changing the degree of interdigitation and/or the molecular conformation.

6. Experimental

6.1. *Characterization*

The chemical structures of the synthesized compounds were assigned by spectroscopic methods and elemental analysis. Proton nuclear magnetic resonance (^{1}H NMR) spectrometry was carried out with a Bruker DRX500 nuclear magnetic resonance spectrometer using $CDCl_3$ as the solvent and TMS as the internal standard. MS spectra were measured with a JEOL, JMS-700 using the FD/MS method.

Thermal properties of the samples were determined by differential scanning calorimetry (DSC) using a Mac Science DSC-3100 at a heating/cooling scan rate of $2\,\mathrm{K\,min^{-1}}$. Texture observation with polarizing optical microscopy (POM) was performed using an Olympus BX-50 equipped with a Linkam hot stage LK-600PH. X-ray diffraction (XRD) measurements were carried out with monochromatic CuK_α radiation of wavelength 1.54 Å from an X-ray generator Bruker AXS D8-Discover with a power of 1.6 kW (40 mA × 40 kV). A two-dimensional position-sensitive detector (Bruker Hi-Star) was used, which had 1024 × 1024 pixels in a $15 \times 15\,\mathrm{cm^2}$ beryllium window.

6.2. *Synthesis procedure*

6.2.1. *4-{5-[2-(Perfluoro-5-methylhexyl)ethoxycarbonyl] pentyloxy}benzoic acid* $\mathbf{4_1}$

A solution of 3 g (15.4 mmol) of 6-bromohexanoic acid in 5 ml of thionyl chloride and 3 drops of dimethylformamide (DMF) was stirred for 24 h at room temperature. Excess thionyl chloride was removed under vacuum and the residue was dissolved in 20 ml methylene chloride (CH_2Cl_2) and 5 ml of tetrahydrofuran (THF). Under ice-cooling, a solution of 6.4 g (15.46 mmol) of 2-(perfluoro-5-methylhexyl)ethanol $\mathbf{1_1}$ and 1.6 g (15.8 mmol) of triethylamine in 20 ml of CH_2Cl_2 and 5 ml of THF was added dropwise over 1.5 h, and the mixture was stirred at room temperature overnight. The solvent was then evaporated and the residue extracted with diethyl ether

(200 ml). After filtration the ether solution was washed with 10% aqueous sodium hydroxide (NaOH) and 20% aqueous sodium chloride (NaCl); the organic layer was dried over $NaSO_4$ and concentrated. The residue (crude $\mathbf{2_1}$) was dissolved in 100 ml of acetone to which 3.5 g of benzyl *p*-hydroxybenzoate and 8 g of potassium carbonate (K_2CO_3) were added. The mixture was stirred at 50°C for 3 days. The solvent was then evaporated and the residue dissolved in 150 ml of ethyl ether and washed with 10% aq. NaOH and 20% aq. NaCl. The organic layer was dried over magnesium sulphate ($MgSO_4$) and then concentrated. Purification was carried out by column chromatography (eluent: ethyl acetate/hexane = 1/4) to obtain the precursor ester $\mathbf{3_1}$ (6.6 g, 58%). The 6.6 g of $\mathbf{3_1}$ was then dissolved in a mixture of 40 ml ethanol and 80 ml ethyl acetate, in which 0.6 g of palladium on activated carbon (Pd/C) was added. Under slight pressure of hydrogen (H_2) hydrogenation was performed to yield the product $\mathbf{4_1}$. After recrystallization from ethanol, 4.9 g of $\mathbf{4_1}$ was obtained (85%).

$\mathbf{4_1}$: Elemental analysis: found, C40.9, H3.1, F44.8; calc. for $C_{22}H_{19}F_{15}O_5 = 648.34$, C40.75, H2.95, F43.95. ^{1}H NMR ($CDCl_3$, 400 MHz, δ/ppm): 1.53 (m, 2H, methylene), 1.72 (q, 2H, methylene), 1.83 (q, 2H, methylene), 2.38 (t, 2H, –OOCCH$_2$–), 2.42–2.53 (m, 2H, –CF$_2$CH$_2$–), 4.03 (t, 2H, –CH$_2$–O–), 4.38 (–COOCH$_2$–), 6.91 (d, 2H, aromatic H), 8.05 (d, 2H, aromatic H), 12 (bs, 1H, –COOH).

6.2.2. *4-{5-[1H, 1H-2,5-di(trifluoromethyl)-3,6-dioxaundecafluorononyloxycarbonyl] pentyloxy}benzoic acid* $\mathbf{4_2}$

A similar procedure to the above-described for $\mathbf{4_1}$ was performed to synthesize $\mathbf{4_2}$. 3 g (15.4 mmol) of 6-bromohexanoic acid, 5 ml of thionyl chloride, 3 drops of DMF, 6.2 g (12.9 mmol) of 1*H*,1*H*-2,5-di(trifluoromethyl)-3,6-dioxaundecafluoro nonanol $\mathbf{1_2}$, 1.6 g of triethylamine, 6.2 g of benzyl *p*-hydroxybenzoate, 8 g of K_2CO_3 were used. The precursor ester $\mathbf{3_2}$ was obtained and purified by column chromatography (ethyl acetate/hexane = 1/5) to yield the precursor ester $\mathbf{3_2}$ (7.1 g, 57.5%), which was hydrogenated using 0.71 g of Pd/C under H_2 to yield 6 g of the acid $\mathbf{4_2}$ (95%).

$\mathbf{4_2}$: Elemental analysis: found C37.0, H2.5, F41.7; calc. for $C_{22}H_{17}F_{17}O_7 = 716.32$, C36.89, H2.39, F45.09. MS $m/z = 716$ (M^+). ^{1}H NMR ($CDCl_3$, 400 MHz, δ/ppm): 1.53 (m, 2H, methylene), 1.74 (q, 2H, methylene), 1.83 (q, 2H, methylene), 2.43 (t, 2H, –OOCCH$_2$–), 4.03 (t, 2H, –CH$_2$–O–), 4.58–4.72 (m, 2H, –CF$_2$CH$_2$–), 6.92 (d, 2H, aromatic H), 8.05 (d, 2H, aromatic H), 12 (bs, 1H, –COOH).

6.2.3. *4-Hydroxylphenyl 4-{5-[2-(perfluoro-5-methylhexyl) ethoxycarbonyl]pentyloxy}benzoate* $\mathbf{7_1}$

A solution of $\mathbf{4_1}$ (2.5 g, 3.86 mmol), 4-(benzyloxy)-phenol (0.772 g, 3.86 mmol), DCC (0.796 g, 3.86 mmol) and DMAP (40 mg, 0.1 eq.) in 40 ml dry CH_2Cl_2 was stirred at room temperature overnight. The precipitate was filtered off and the filtrate concentrated. The residue was purified by column chromatography (ethyl acetate/hexane = 1/3) to yield 2 g of the precursor $\mathbf{5_1}$ (62%). Then 1.85 g of the benzyl ester $\mathbf{5_1}$ was hydrogenated using 0.19 g of Pd/C under a slight pressure of H_2 in a mixed solvent of ethanol and ethyl acetate to yield the product $\mathbf{7_1}$ (1.6 g, 97%).

$\mathbf{5_1}$: Elemental analysis: found, C50.8, H3.3, F34.0%; calc. for $C_{35}F_{15}H_{29}O_6 = 830.58$, C50.61, H3.52, F34.31%. MS $m/z = 830$ (M^+). ^{1}H NMR ($CDCl_3$, 400 MHz, δ): 1.53 (m, 2H, methylene), 1.73 (q, 2H, methylene), 1.85 (q, 2H, methylene), 2.39 (t, 2H, –OOC–CH$_2$–), 2.45–2.54 (m, 2H, methylene), 4.04 (t, 2H, –CH$_2$–O–ϕ–), 4.39 (t, 2H, –CH$_2$–OOC–), 5.07 (s, 2H, –OCH$_2$–ϕ), 6.95 (d, 2H, ArH of –O–ϕ–COO–), 7.06 (dd, 4H, ArH of –COO–ϕ–O–), 7.33–7.45 (m, 5H, ArH of –CH$_2$–ϕ), 8.13 (d, 2H, ArH of –O–ϕ–COO–). $\mathbf{7_1}$: Elemental analysis: found, C45.8, H3.0, F38.1; calc. for $C_{28}F_{15}H_{23}O_6 = 740.46$, C45.42, H3.13, F38.49%. MS $m/z = 740$ (M^+). ^{1}H NMR ($CDCl_3$, 400 MHz, δ/ppm): 1.53 (m, 2H, methylene), 1.73 (q, 2H, methylene), 1.85 (q, 2H, methylene), 2.39 (t, 2H, –OOC–CH$_2$–), 2.43–2.54 (m, 2H, methylene), 4.04 (t, 2H, –CH$_2$–O–ϕ–), 4.39 (t, 2H, –CH$_2$–OOC–), 4.93 (s, 1H, –OH), 6.84 (d, 2H, ArH of –O–ϕ–COO–), 7.00 (dd, 4H, ArH of –COO–ϕ–O–), 8.12 (d, 2H, ArH of –O–ϕ–COO–).

6.2.4. *4-Hydroxyphenyl 4-{5-[1H-2,5-di(trifluoromethyl)-3,6-dioxaundecafluorononyloxycarbonyl]pentyloxy} benzoate* $\mathbf{7_2}$

A solution of $\mathbf{4_2}$ (3 g, 5.02 mmol), 4-(benzyloxy)-phenol (1 g, 5.02 mmol), DCC (1.04 g, 5.02 mmol) and DMAP (61 mg, 0.1 eq.) in 45 ml dry CH_2Cl_2 was stirred at room temperature overnight. The precipitate was filtered off and the filtrate concentrated. The residue was purified by column chromatography (ethyl acetate/hexane = 1/3) to yield 2.45 g of the precursor ester $\mathbf{5_2}$ (65%), which was hydrogenated using 0.25 g of Pd/C under a slight pressure of H_2 in a solvent of ethanol and ethyl acetate, yielding $\mathbf{7_2}$ (2 g, 91%).

$\mathbf{5_2}$: Elemental analysis: found, C47.1, H2.8, F35.5; calc. for $C_{35}F_{17}H_{27}O_8 = 898.57$, C = 46.78, H = 3.03, F = 35.95. (MS $m/z = 898$ (M^+). ^{1}H NMR ($CDCl_3$, 400 MHz, δ/ppm): 1.54 (m, 2H, methylene), 1.74 (q, 2H, methylene), 1.85 (q, 2H, methylene), 2.45 (t, 2H, –OOC–CH$_2$–), 4.04 (t, 2H, –CH$_2$–O–ϕ–), 4.65 (q, 2H, –CF$_2$–CH$_2$–OOC–), 5.07 (s, 2H, –OCH2–ϕ), 6.95 (d,

2H, ArH of –O–ϕ–COO–), 7.06 (dd, 4H, ArH of –COO–ϕ–O–), 7.33–7.46 (m, 5H, ArH of $–CH_2–ϕ$), 8.13 (d, 2H, ArH of –O–ϕ–COO–). **7_2**: Elemental analysis: found, C 42.2, H 2.5, F 38.8; calc. for $C_{28}F_{17}H_{21}O_8 = 808.45$, C 41.60, H 2.62, F 39.95%. MS $m/z = 808$ (M^+). ^{1}H NMR ($CDCl_3$, 400 MHz, δ/ppm): 1.54 (m, 2H, methylene), 1.74 (q, 2H, methylene), 1.85 (q, 2H, methylene), 2.45 (t, 2H, $–OOC–CH_2–$), 4.04 (t, 2H, $–CH_2–O–ϕ–$), 4.66 (q, 2H, $CF–CH_2–OOC–$), 6.84 (d, 2H, ArH of –O–ϕ–COO–), 7.00 (dd, 4H, ArH of –COO–ϕ–O–), 8.13 (d, 2H, ArH of –O–ϕ–COO–).

6.2.5. *4-(Carboxy)phenyl 4-{5-[2-(perfluoro-5-methylhexyl) ethoxycarbonyl]pentyloxy}benzoate* ***8_1***

A solution of 1 g (1.54 mmol) of **4_1**, 0.35 g (1.54 mmol) of benzyl *p*-hydroxybenzoate, 0.32 g (1.54 mmol) of DCC and 0.02 g (0.15 mmol) of DMAP in 25 ml dry CH_2Cl_2 and 1 ml dry THF was stirred at room temperature overnight. The precipitate was filtered off, and the filtrate concentrated. The residue was purified by column chromatography (ethyl acetate/hexane = 1/4) to yield 0.97 g of the precursor ester **6_1** (73%). Then 0.6 g (0.7 mmol) of **6_1** was hydrogenated using 0.06 g of Pd/C under a slight pressure of H_2 in a mixture of ethanol and ethyl acetate to yield 0.46 g of **8_1** (87%).

6_1: Elemental analysis: found, C50.9, H3.5, F32.4; calc. for $C_{36}H_{29}O_7F_{15} = 858.59$, C50.36, H3.40, F33.19%. MS $m/z = 858$ (M^+). ^{1}H NMR ($CDCl_3$, 400 MHz, δ/ppm): 1.55 (m, 2H, methylene), 1.73 (q, 2H, methylene), 1.85 (q, 2H, methylene), 2.39 (t, 2H, $–OOCCH_2–$), 2.43–2.54 (m, 2H, $–CF_2CH_2–$), 4.05 (t, 2H, $–CH_2–O–$), 4.39 (t, 2H, $–COOCH_2–$), 5.38 (s, 2H, $–CH_2–ϕ–$), 6.96 (dd, 2H, aromatic), 7.29 (dd, 2H, aromatic), 7.35–7.47 (m, 5H, aromatic H), 8.13 (dd, 2H, aromatic H), 8.16 (dd, 2H, aromatic H). **8_1**: Elemental analysis: found, C 45.9, H 3.2, F 36.6; calc. for $C_{29}H_{23}O_7F_{15} = 768.47$, C 45.32, H 3.02, F 37.09. MS $m/z = 768$ (M^+). ^{1}H NMR ($CDCl_3$, 400 MHz, δ/ppm): 1.54 (m, 2H, methylene), 1.74 (q, 2H, methylene), 1.86 (q, 2H, methylene), 2.39 (t, 2H, $–OOCCH_2–$), 2.43–2.54 (m, 2H, $–CF_2CH_2–$), 4.06 (t, 2H, $–CF_2CH_2–$), 4.39 (t, 2H, $–COOCH_2–$), 6.97 (dd, 2H, aromatic), 7.34 (d, 2H, aromatic), 8.14 (dd, 2H, aromatic H), 8.19 (d, 2H, aromatic H).

6.2.6. *4-(Carboxy)phenyl 4-{5-[1H,1H-2,5-di (trifluoromethyl)-3,6-dioxaundecafluorononyloxycarbonyl] pentyloxy}benzoate* ***8_2***

A solution of 3 g (4.2 mmol) of **4_2**, 0.96 g (4.2 mmol) of benzyl *p*-hydroxybenzoate, 0.864 g (4.2 mmol) of DCC and 0.052 g (0.42 mmol) of DMAP in 30 ml dry CH_2Cl_2 and 3 ml dry THF was stirred at room temperature overnight. The precipitate was filtered off and the filtrate concentrated. The residue was purified by column chromatography (ethyl acetate/hexane = 1/5) and recrystallized from methanol to yield 3.1 g of the precursor ester **6_2** (88.4%). Then **6_2** (1.5 g, 1.62 mmol) was hydrogenated using 0.15 g of Pd/C under a slight pressure of H_2 in a mixture of ethanol and ethyl acetate to yield 1.2 g of **8_2** (68.5%).

6_2: Elemental analysis: found, C46.7, H2.90, F34.4; calc. for $C_{36}H_{27}O_9F_{17} = 926.58$, C46.66, H2.94, F34.86%. MS $m/z = 926$ (M^+). ^{1}H NMR ($CDCl_3$, 400 MHz, δ/ppm): 1.54 (q, 2H, methylene), 1.74 (q, 2H, methylene), 1.87 (q, 2H, methylene), 2.45 (t, 2H, $–OOCCH_2–$), 4.04 (t, 2H, $–CH_2–O–$), 4.59–4.72 (m, 2H, $–CF_2CH_2–$), 6.96 (dd, 2H, aromatic H), 7.29 (dd, 2H, aromatic H), 7.35–7.46 (m, 5H, aromatic H), 8.13 (dd, 2H, aromatic H), 8.14 (dd, 2H, aromatic H). **8_2**: Elemental analysis: found, C 41.7, H 2.5%, calc. for $C_{29}H_{21}F_{17}O_9 = 836.45$, C 41.64, H 2.53, F 38.62%. MS $m/z = 836$ (M^+). ^{1}H NMR ($CDCl_3$, 400 MHz, δ/ppm): 1.53 (m, 2H, methylene), 1.74 (m, 2H, methylene), 1.83 (m, 2H, methylene), 2.43 (t, 2H, $–OOCCH_2–$), 4.03 (t, 2H, $–CH_2–O–$), 4.58–4.72 (m, 2H, $–CF_2CH_2–$), 6.92 (d, 2H, aromatic H), 7.35 (d, 2H, aromatic H), 8.15 (d, 2H, aromatic H), 8.20 (d, 2H, aromatic H).

6.2.7. *Preparation of the acid/base hydrogen-bonded complexes between the acids* ***4_n*** *and 4,4′-dipyridyl*

In the general procedure used to prepare acid/base hydrogen-bonded complexes, a 2 : 1 molar ratio of one of the acids (**4_n**) and 4,4′-dipyridyl was dissolved in dry THF. The solvent was then removed by heating and the residue further heated to melt into an isotropic liquid; it was then cooled to ambient temperature.

References

[1] (*a*) Goodby, J. W., Bruce, D. W., Hird, C., Imrie, C., and Neal, M., 2001, *J. mater. Chem.*, **11,** 2631; (*b*) Tschierske, C., 2001, *J. mater. Chem.*, **11,** 2647; (*c*) Fazio, D., Mongin, C., Donnio, B., Galerne, Y., Guillon, D., and Bruce, D., 2001, *J. mater. Chem.*, **11,** 2852; (*d*) Lee, M., Cho, B.-K., and Zin, W.-C., 2001, *Chem. Rev.*, **101,** 3869.

[2] (*a*) Tournilhac, F., Blinov, L. M., Simon, J., and Yablonsky, S. V., 1992, *Nature*, **359,** 621; (*b*) Höpken, J., Pugh, C., Richtering, W., and Möller, M., 1988, *Makromol. Chem.*, **189,** 911; (*c*) Nguyen, H. T., Sigaud, G., Achard, M. F., Hardouin, F., Twieg, R. J., and Betterton, K., 1991, *Liq. Cryst.*, **10,** 389; (*d*) Rieker, T. P., and Janulis, E. P., 1995, *Phys. Rev. E*, **52,** 2688; (*e*) Kromm, P., Cotrait, M., and Nguyen, H. T., 1996, *Liq. Cryst.*, **21,** 95; (*f*) Diele, S., Lose, D., Kruth, H., Pelzl, G., Guittard, F., and Cambon, A., 1996, *Liq. Cryst.*, **21,** 603; (*g*) Lobko, T. A., Ostrovskii, B. I., Pavluchenko, A. I., and Sulianov, S. N., 1993, *Liq. Cryst.*, **15,** 361; (*h*) Arehart, S. V., and Pugh, C., 1997, *J. Am. chem. Soc.*, **119,** 3027; (*i*) Liu, H., and Nohira, H., 1997, *Liq. Cryst.*, **22,** 217; (*j*) Yang, X., Abe, K., Kato, R., Yano, S., Kato, T., Miyazawa, K.,

and TAKEUCHI, H., 1998, *Liq. Cryst*., **25,** 639; (*k*) SMALL, A. C., HUNT, D. K., and PUGH, C., 1999, *Liq. Cryst*., **26,** 849; (*l*) PETROV, V. F., DUAN, M., OKAMOTO, H., MU, J., SHIMIZU, Y., and TAKENAKA, S., 2001, *Liq. Cryst*., **28,** 387; (*m*) YANG, Y.-G., and WEN, J.-X., 2001, *Liq. Cryst*., **28,** 1735.

[3] KÖLBEL, M., BEYERSDORFF, T., CHENG, X. H., TSCHIERSKE, C., KAIN, J., and DIELE, S., 2001, *J. Am. chem. Soc.*, **123,** 6809.

[4] KATO, T., and FRÉCHET, J. M. J., 1989, *J. Am. chem. Soc.*, **111,** 8533.

[5] (*a*) KATO, T., 2000, *Struct. Bond.*, **96,** 95; (*b*) PALEOS, C. M., and TSIOURVAS, D., 2001, *Liq. Cryst*., **28,** 1127.

[6] NISHIKAWA, E., YAMAMOTO, J., and YOKOYAMA, H., 2001, *Chem. Lett*., 454.

[7] NISHIKAWA, E., YAMAMOTO, J., and YOKOYAMA, H. in *Advances in Liquid Crystalline Materials and Technologies*, edited by P. T. Mather, D. J. Broer, T. J. Bunning, D. M. Walba, and R. Zentel, 2001, *MRS Symposium Proceedings*, Vol. 709, p. 241.

[8] KATO, T., FRÉCHET, M. J., WILSON, P. G., SAITO, T., URYU, T., FUJISHIMA, A., JIN, C., and KANEUCHI, F., 1993, *Chem. Mater.*, **5,** 1094.

[9] (*a*) SCHWARZ, U. S., and GOMPPER, G., 1999, *Phys. Rev. E*, **59,** 5528; (*b*) BENEDICTO, A. D., and O'BRIEN, F., 1997, *Macromolecules*, **30,** 3395.

[10] (*a*) SQUIRES, A., TEMPLER, R. H., CES, O., GABKE, A., WOENCKHAUS, J., SEDDON, J. M., and WINTER, R., 2000, *Langmuir*, **16,** 3578; (*b*) SAKURAI, S., ISOBE, D., OKAMOTO, S., YAO, T., and NOMURA, S., 2001, *Phys. Rev. E*, **63,** 061803.

[11] KUTSUMIZU, S., ICHIKAWA, T., YAMADA, M., NOJIMA, S., and YANO, S., 2000, *J. Phys. Chem. B*, **104,** 10196.

[12] DONNIO, B., HEINRICH, B., GULIK-KRZYWICKI, T., DELACROIX, H., GUILLON, D., and BRUCE, D. W., 1997, *Chem. Mater.*, **91,** 2951.

[13] GRAY, G. W., JONES, B., and NARSON, F., 1957, *J. chem. Soc*., 393.

[14] DEMUS, D., KUNICKE, G., KEELSEN, J., and SACKMANN, A., 1968, *Z. Naturforsch.*, **23a,** 84.

[15] GRAY, G. W., and GOODBY, J. W., 1984, *Smectic Liquid Crystals* (Leonard Hill), pp. 68–81.

[16] KUTSUMIZU, S., YAMADA, M., and YANO, S., 1994, *Liq. Cryst.*, **16,** 1106.

[17] UKLEJA, P., SIATKOWSKI, R. E., and NEUBERT, M. E., 1988, *Phys. Rev. A*, **38,** 4815.

[18] TANSHO, M., ONODA, Y., KATO, R., KUTSUMIZU, S., and YANO, S., 1998, *Liq. Cryst.*, **24,** 525.

[19] KUTSUMIZU, S., KATO, R., YAMADA, M., and YANO, S., 1997, *J. Phys. Chem. B*, **101,** 10666.

[20] KUTSUMIZU, S., YAMAGUCHI, T., KATO, R., and YANO, S., 1999, *Liq. Cryst.*, **26,** 567.

[21] RAO, D. S. S., PRASAD, S. K., PRASAD, V., and KUMAR, S., 1999, *Phys. Rev. E*, **59,** 5572.

[22] (*a*) SAITO, K., SATO, A., and SORAI, M., 1998, *Liq. Cryst*., **25,** 525; (*b*) SAITO, K., SHINHARA, T., and SORAI, M., 2000, *Liq. Cryst*., **27,** 1555.

[23] MAEDA, Y., CHENG, G., KUTSUMIZU, S., and YANO, S., 2001, *Liq. Cryst.*, **28,** 1785.

[24] MALTHÊTE, J., NGUYEN, H. T., and DESTRADE, C., 1993, *Liq. Cryst.*, **13,** 17.

[25] DEMUS, D., GOODBY, J., GRAY, W. G., SPIESS, H.-W., VILL, V., (editors), 1998, *Handbook of Liquid Crystals* (Weinheim: Wiley-VCH).

[26] (*a*) YOSHIZAWA, A., UMEZAWA, J., ISE, N., SATO, R., SOEDA, Y., KUSUMOTO, T., SATO, K., HIYAMA, T., TAKANISHI, Y., and TAKEZOE, H., 1998, *Jpn. J. appl. Phys*., **37,** 942; (*b*) TAKANISHI, Y., OGASAWARA, T., YOSHIZAWA, A., UMEZAWA, J., KUSUMOTO, T., HIYAMA, T., ISHIKAWA, K., and TAKEZOE, H., 2002, *J. mater. Chem*., **12,** 1.

[27] BALAGURUSAMY, V. S. K., UNGAR, G., PERCEC, V., and JOHANSSON, G., 1997, *J. Am. Chem. Soc.*, **119,** 1539.

[28] KANIE, K., NISHII, M., YASUDA, T., TAKI, T., UJIIE, S., and KATO, T., 2001, *J. mater. Chem.*, **11,** 2875.

[29] BORISCH, K., TSCHIERSKE, C., GÖRING, P., and DIELE, S., 2000, *Langmuir*, **16,** 6701.

[30] GUILLEVIC, M.-A., GELBRICH, T., HURSTHOUSE, M. B., and BRUCE, D., 2001, *Mol. Cryst. Liq. Cryst.*, **362,** 147.

[31] (*a*) NISHIKAWA, E., and SAMULSKI, E. T., 2000, *Liq. Cryst*., **27,** 1463; (*b*) SUNOHARA, K., TAKATO, K., and SAKAMOTO, M., 1993, *Liq. Cryst*., **13,** 283; (*c*) VIETH, C. A., SAMULSKI, E. T., and MURTHY, N. S., 1995, *Liq. Cryst*., **19,** 557; (*d*) PUGH, C., BAE, J.-Y., DHARIA, J., Ge., J.-J., and CHENG, S. Z. D., 1998, *Macromolecules*, **31,** 5188.

[32] LEE, M., CHO, B., KANG, Y.-S., and ZIN, W.-C., 1999, *Macromolecules*, **32,** 8531.

[33] YONEYA, M., NISHIKAWA, E., and YOKOYAMA, H., 2002, *J. Chem. Phys.*, **116,** 5753.

[34] NISHIKAWA, E., YAMAMOTO, J., and YOKOYAMA, H., 2001, *Chem. Lett*., 94.

[35] private result.

[36] (*a*) GÖRING, P., DIELE, S., FISCHER, S., WIEGELEBEN, A., PELZL, G., STEGEMEYER, H., and THYEN, W., 1998, *Liq. Cryst*., **25,** 467; (*b*) MORIMOTO, N., SAITO, K., MORITA, Y., NAKASUJI, K., and SORAI, M., 1999. *Liq. Cryst*., **26,** 219.

[37] DE GENNES, P. G., and PROST, J., 1993, *The Physics of Liquid Crystals* (Oxford: Clarendon Press).

[38] ALAPATI, P. R., ARULSANKAR, A., GOGOI, B., GHOSH, T. K., and NAGAPPA, 2001, *Mol. Cryst. Liq. Cryst.*, **366,** 61.

[39] (*a*) RATNA, B. R., SHASHIDHAR, R., GEETHA, G. N., PRASAD, S. K., BAHR, CH., and HEPPKE, G., 1988, *Phys. Rev. A*, **37,** 1824; (*b*) BAHR, CH., and HEPPKE, G., 1986, *Mol. Cryst. Liq. Cryst*., **148,** 29.

[40] LIEN, S. C., and HUANG, C. C., 1984, *Phys. Rev. A*, **30,** 624.

[41] (*a*) LIU, H. Y., HUANG, C. C., MIN, T., WAND, M. D., WALBA, D. M., CLARK, N. A., BAHR, CH., and HEPPKE, G., 1989, *Phys. Rev. A*., **40,** 6759; (*b*) LIU, H. Y., HUANG, C. C., BAHR, CH., and HEPPKE, 1988, *Phys. Rev. Lett*., **61,** 345; (*c*) DAS, P., EMA, K., and GARLAND, C. W., 1989, *Liq. Cryst*., **4,** 205; (*f*) ALAPATI, P. R., ARULSANKAR, A., GOGOI, B., GHOSH, T. K., and NAGAPPA, 2001, *Mol. Cryst. Liq. Cryst*., **366,** 61; (*d*) BAHR, CH., and HEPPKE, G., 1990, *Phys. Rev. A*, **41,** 4335.

[42] (*a*) RADCLIFFE, M. D., BROSTROM, M. L., EPSTEIN, K. A., RAPPAPORT, A. G., THOMAS, B. N., SHAO, R., and CLARK, N. A., 1999, *Liq. Cryst*., **26,** 789; (*b*) IANNACCHIONE, G. S., GARLAND, C. W., JOHNSON, P. M., and HUANG, C. C., 1999, *Liq. Cryst*., **26,** 51; (*c*) TANG, A., KONOVALOV, D., NACIRI, J., RATNA, B. R., and SPRUNT, S., 2001, *Phys. Rev. E*, **65,** 010703–1; (*d*) EREMIN, A., DIELE, S., PELZL, G., KOVALENKO, L.,

PELZ, K., and WEISSFLOG, W., 2001, *Liq. Cryst*., **28,** 1451.
[43] LOSE, D., DIELE, S., DIETZMANN, E., and WEISSFLOG, W., 1998, *Liq. Cryst.*, **24,** 707.
[44] JANG, W. G., GLASER, M. A., PARK, C. S., KIM, K. H., LANSAC, Y., and CLARK, N. A., 2001, *Phys. Rev. E*, **64,** 051712–1.
[45] SPECTOR, M. S., HEINEY, P. A., NACIRI, J., WESLOWSKI, B. T., HOLT, D. B., and SHASHIDHA, R., 2000, *Phys. Rev. E*, **61,** 1579.
[46] DE VRIES, A., 1977, *Mol. Cryst. liq. Cryst. Lett.*, **41,** 27.
[47] TOURNILHAC, F. G., BOSIO, L., SIMON, J., BLINOV, L. M., and YABLONSKY, S. V., 1993, *Liq. Cryst.*, **14,** 405.
[48] NISHIKAWA, E., YAMAMOTO, J., and YOKOYAMA, H., 2003, *Chem. Commun*., 420.